Effects of dynamical and structural modifications on synchronization

Cite as: Chaos **29**, 083131 (2019); https://doi.org/10.1063/1.5110727
Submitted: 20 May 2019 . Accepted: 06 August 2019 . Published Online: 30 August 2019

Lijia Chen, Peng Ji, David Waxman, Wei Lin, and Juergen Kurths

Effects of dynamical and structural modifications on synchronization

Cite as: Chaos **29**, 083131 (2019); doi: 10.1063/1.5110727
Submitted: 20 May 2019 · Accepted: 6 August 2019 ·
Published Online: 30 August 2019

Lijia Chen,[1,2,3] Peng Ji,[1,2,3,a)] David Waxman,[1,2] Wei Lin,[1,2,3,4] and Juergen Kurths[5,6]

AFFILIATIONS

[1]Institute of Science and Technology for Brain-Inspired Intelligence, Fudan University, Shanghai 200433, China
[2]LCNBI and LMNS (Fudan University), Ministry of Education, Shanghai 200433, China
[3]Research Institute of Intelligent and Complex Systems, Fudan University, Shanghai 200433, China
[4]School of Mathematical Sciences and Centre for Computational Systems Biology, Fudan University, Shanghai 200433, China
[5]Potsdam Institute for Climate Impact Research, 14473 Potsdam, Germany
[6]Department of Physics, Humboldt University, 12489 Berlin, Germany

Note: This paper is part of the Focus Issue on Symmetry and Optimization in the Synchronization and Collective Behavior of Complex Systems.
[a)]**Electronic mail:** pengji@fudan.edu.cn

ABSTRACT

Synchronization is a phenomenon of the collective behavior of coupled oscillators and involves the detailed interplay of the intrinsic frequencies of the oscillators, the underlying topological features of their interaction network, and external perturbations. In this work we investigate, in the strong coupling regime, the response of a system to external perturbations of its natural frequencies and network modifications. Our investigation relies on two performance measures (one for phases and the other for frequencies) and a spectral perturbation analysis. Given strongly localized perturbations in time, corresponding to the dominant eigenmode of the weighted Laplacian matrix of the network, we present a sufficient condition for the maximization of the system's stability, along with analytical results for the effects of structural perturbations on the system's response. A number of simulations are conducted to illustrate the theory presented.

The study of network synchronization in various systems is useful to deepen our understanding of how to optimize robustness and predict the effects of internal and external disturbances. Whether a disturbed system's performance can be solely predicted from the underlying spectrum of its network remains an open question. In this work, which is based on the classical Kuramoto model, we adopt two existing performance measures. These enable us to quantify the integrated variance of a system's states and reveal the rate at which the system returns to the synchronized state. In particular, we provide analytical expressions of both response measures, one for phases, the other for frequencies, in the basin of attraction of the synchronized state, given external (structural) and internal (dynamical) perturbations. Our analysis shows that a system's return rate can be minimized or maximized given temporally localized (Dirac delta) perturbations, corresponding to different eigenmodes of the Laplacian matrix of the network, thereby enriching our ability to understand and predict the return-rate of a system after structural perturbations.

I. INTRODUCTION

The phenomenon of synchronization can be found in many natural and technological systems[1–3] where a level of coherence plays an important role, e.g., in neutrino oscillations in matter,[4] in cascading failures of power grids,[5] and in the phase locking of Josephson-junction series arrays.[6,7] The main focus of the study of synchronization of complex systems is to understand how collective behavior emerges from a collection of coupled oscillators, and multidisciplinary perspectives/approaches have been used to make progress.[8,9] The present work is based on the Kuramoto model, which was originally motivated by biological systems,[10] and involves nonlinear interactions of coupled oscillators. It has become a classic model in this area.[1–3] The degree of synchronization of this model, as measured by two existing performance measures of the dynamical response of the system, can be influenced by spectral properties of the complex topology, for example, the largest eigenvalue and the dominant eigenmode of the Laplacian matrix.[3,11]

Given the widespread applications and importance of synchronization, it is important to develop analytical tools that can enhance

our understanding of the collective behavior of coupled heterogeneous oscillators. Here, we investigate two performance measures of robustness, one for the phases, the other for the frequencies, in the Kuramoto model. These measures characterize a system's response to external perturbations inside the basin of attraction of the synchronized state.[12–15] This line of research has been previously explored via a master stability function for identical oscillators, given small dynamical perturbations,[16] the basin stability for nonidentical oscillators given large perturbations,[17,18] and a synchrony alignment function under structural modifications.[19]

In this paper, we conduct an analysis of the robustness of synchronization, in the strong coupling regime, by taking into account a system's response to dynamical and structural perturbations. In Sec. II, we introduce the Kuramoto phase oscillator model along with two response measures in the basin of attraction of the synchronized state, one measure for the phases and the other for the rate of change of the phases. In Sec. III, we derive analytical expressions for both performance measures, as a function of the perturbation and the spectral properties of the underlying Laplacian matrix. We derive a sufficient condition to optimize the system's return to synchronization. In Sec. IV, we approximate both performance measures when there are structural modifications.

II. SYSTEM DYNAMICS

We consider a system consisting of N nonlinearly coupled oscillators, where the dynamical variable of the ith oscillator is the phase θ_i, with $i = 1, 2, \ldots, N$. The time evolution of oscillator i is governed by the classical Kuramoto model,

$$\dot{\theta}_i = \omega_i + K \sum_{j=1}^{N} \boldsymbol{A}_{ij} \sin(\theta_j - \theta_i), \quad i = 1, 2, \ldots, N. \tag{1}$$

Here, $\dot{\theta}_i = d\theta_i/dt$, ω_i is the natural frequency of the ith oscillator, while $\boldsymbol{A}_{ij} = 1$ if oscillator i is coupled to oscillator j and $\boldsymbol{A}_{ij} = 0$ if these oscillators are uncoupled. The $\boldsymbol{A}_{ij}$ constitute elements of a symmetric adjacency matrix $\boldsymbol{A}$ ($\boldsymbol{A}_{ij} = \boldsymbol{A}_{ji}$), that is, associated with an undirected connectivity graph of the oscillators. The sum of all natural frequencies is equal to zero and, in the strong coupling regime, all oscillators are synchronized without rotation.

The overall coupling strength K appearing in Eq. (1) plays a crucial role in the collective dynamics of the coupled oscillators. It is well-known that there is a critical value of the coupling strength, K_c, such that for $K < K_c$ the oscillators behave incoherently, but for $K > K_c$ the oscillators generally exhibit a partial level of synchronization, and for sufficiently large K the oscillators reach a stable synchronized state, where all phases change with the same frequency.[1–3] Here, we work under the assumption that all oscillators are located in the regime of the stable synchronized state, whose phases we collectively represent by $\theta^{(0)} = (\theta_1^{(0)}, \theta_2^{(0)}, \ldots, \theta_N^{(0)})^T$ (a T superscript denotes a matrix transpose), when the natural frequencies of the oscillators are collectively given by $\omega^{(0)} = (\omega_1^{(0)}, \omega_2^{(0)}, \ldots, \omega_N^{(0)})^T$. For the stable synchronized state, we thus have

$$0 = \omega_i^{(0)} + K \sum_{j=1}^{N} \boldsymbol{A}_{ij} \sin(\theta_j^{(0)} - \theta_i^{(0)}). \tag{2}$$

To evaluate a system's behavioral response in the strong coupling regime, we introduce time-dependent perturbations of the natural frequencies, by writing $\omega_i(t) = \omega_i^{(0)} + \delta\omega_i(t)$, where the perturbation $\delta\omega_i(t)$ is 0 for $t < 0$ and nonzero for $t \geq 0$. The resulting phases are generally time-dependent, so we write $\theta_i(t) = \theta_i^{(0)} + \delta\theta_i(t)$. Substituting these forms for $\omega_i(t)$ and $\theta_i(t)$ into Eq. (1) yields

$$\delta\dot{\theta}_i(t) = \delta\omega_i(t) + K \sum_{j=1}^{N} \boldsymbol{A}_{ij} \cos(\theta_i^{(0)} - \theta_j^{(0)}) \delta\theta_j - K \sum_{j=1}^{N} \boldsymbol{A}_{ij} \cos(\theta_i^{(0)} - \theta_j^{(0)}) \delta\theta_i, \quad i = 1, 2, \ldots, N,$$

and by linearization, we obtain

$$\delta\dot{\boldsymbol{\theta}}(t) = \delta\boldsymbol{\omega}(t) - \boldsymbol{L}(\theta^{(0)})\delta\theta, \tag{3}$$

where $\boldsymbol{L}(\theta^{(0)})$ is the Laplacian matrix which is calculated as follows

$$\boldsymbol{L}_{ij} = \begin{cases} -K \cos(\theta_i^{(0)} - \theta_j^{(0)}) & \text{when } i \neq j, \\ K \sum_k \boldsymbol{A}_{jk} \cos(\theta_j^{(0)} - \theta_k^{(0)}) & \text{when } i = j. \end{cases} \tag{4}$$

We now consider two existing performance-measures that capture the robustness of the synchronized state and allow us to quantify the dynamical response of the system to perturbations.[12–15] These are

$$H_1(T) = \sum_{i=1}^{N} \int_0^T [\delta\theta_i(t) - \Delta(t)]^2 dt, \tag{5}$$

$$H_2(T) = \sum_{i=1}^{N} \int_0^T \left[\delta\dot{\theta}_i(t) - \dot{\Delta}(t)\right]^2 dt, \tag{6}$$

where

$$\Delta(t) = \frac{1}{N} \sum_i \delta\theta_i(t). \tag{7}$$

Here, $H_1(T)$ sums the integrated squared differences of phases of different oscillators, from the average phase, over a time-interval of T, while $H_2(T)$ is the corresponding quantity for the frequencies (rates of change of the phases). Both $H_1(T)$ and $H_2(T)$ quantify the degree of a system's dynamical response to perturbations. The measure $H_1(T)$ integrates the phase differences of each node, apart from synchronized states, and is expected to be small if the system is stable under given perturbations, while $H_2(T)$ reflects the system's return rate and is assumed to be large.

Since the Laplacian matrix $\boldsymbol{L}(\theta^{(0)})$ is real and symmetric, its eigenvectors can be chosen as orthonormal. We use u_α to denote the right eigenvector of $\boldsymbol{L}(\theta^{(0)})$ associated with eigenvalue λ_α (with $\alpha = 1, 2, \ldots, N$). The u_α are N component column vectors, and orthonormality corresponds to $u_\alpha^T u_\beta = \delta_{\alpha\beta}$, where $\delta_{\alpha\beta}$ is a Kronecker delta. These eigenvectors form a basis and we can write the set of all phase changes as $(\delta\theta_1, \delta\theta_2, \ldots \delta\theta_N)^T \equiv \delta\theta(t) = \sum_\alpha C_\alpha(t) u_\alpha$, where $C_\alpha(t)$ are a set of scalar coefficients. Use of this representation of $\delta\theta(t)$ allows Eq. (3) to be rewritten as

$$\dot{C}_\alpha(t) = \delta\omega^T(t) u_\alpha - \lambda_a C_\alpha(t) \tag{8}$$

and this has the general solution $C_\alpha(t) = \mathrm{e}^{-\lambda_\alpha t} C_\alpha(0) + \mathrm{e}^{-\lambda_\alpha t} \int_0^t \mathrm{e}^{\lambda_\alpha t'} \delta\omega^T(t') u_\alpha dt'$. As the system is in a stable synchronized state for times

prior to $t = 0$, we can take all $C_\alpha(0) = 0$. Thus

$$C_\alpha(t) = e^{-\lambda_\alpha t} \int_0^t e^{\lambda_\alpha t'} \delta\omega^T(t') u_\alpha dt' \tag{9}$$

and substituting this solution into Eq. (5), we find that the performance function $H_1(T)$, for the phases, becomes

$$H_1(T) = \sum_{\alpha(\neq 1)} \int_0^T [C_\alpha(t)]^2 \, dt, \tag{10}$$

where the sum excludes the contribution associated with zero eigenvalue, whose eigenvector is $u_1 = \frac{1}{\sqrt{N}}(1, 1, \ldots, 1)^T$.

Similarly, after substituting the solution of Eq. (9) into Eq. (6), the other performance function $H_2(T)$, for the frequencies, becomes

$$H_2(T) = \sum_{\alpha(\neq 1)} \int_0^T \left[\dot{C}_\alpha(t)\right]^2 dt. \tag{11}$$

To investigate the combined effects of perturbations on both performance functions [$H_1(T)$ and $H_2(T)$], we shall first consider perturbations of the natural frequencies that are highly localized in time (approximated by Dirac delta perturbations). We note that both measures have previously been investigated via generalized Kirchhoff indices.[15] We additionally investigate structural perturbations on both performance measures via spectra perturbation theory.

III. DIRAC DELTA PERTURBATIONS

The performance measures, $H_1(T)$ and $H_2(T)$, are functions of the $C_\alpha(t)$, which incorporate the spectral properties of the connection network and the perturbed natural frequencies. For a given network, the quantity $\delta\omega$ becomes the crucial variable in $C_\alpha(t)$. In what follows, we shall choose $\delta\omega$ to be highly localized in the vicinity of $t = 0$, which we approximate by a constant times a Dirac delta function of argument t, and we investigate the effects of such a perturbation on the performance measures $H_1(T)$ and $H_2(T)$.

Since $\delta\omega$ is highly localized in the vicinity of $t = 0$, we approximate this by $\delta\omega = \delta\omega_0 \tau_0 \delta(t)$, where $\delta(t)$ is a Dirac delta function of argument t, the quantity τ_0 is a timescale associated with the perturbation, and $\delta\omega_0$ is a column vector of time-independent frequencies. The form that $C_\alpha(t)$ takes [following Eq. (9)] is

$$C_\alpha(t) = \eta_\alpha \tau_0 e^{-\lambda_\alpha t}, \tag{12}$$

where

$$\eta_\alpha = {\delta\omega_0}^T u_\alpha \tag{13}$$

is a time independent scalar and, by assumption, the entire area of the Dirac delta function contributes to the integral in Eq. (9).

Substituting this form of $C_\alpha(t)$ into Eqs. (10) and (11) yields the two performance measures [$H_1(T)$ and $H_2(T)$], as the following functions of the coefficients, η_α, and the timescale, τ_0:

$$\begin{aligned} H_1(T) &= \sum_{\alpha(\neq 1)} \int_0^T \left[\eta_\alpha \tau_0 e^{-\lambda_\alpha t}\right]^2 dt \\ &= \sum_{\alpha(\neq 1)} \eta_\alpha^2 \tau_0^2 f(\lambda_\alpha), \end{aligned} \tag{14}$$

$$\begin{aligned} H_2(T) &= \sum_{\alpha(\neq 1)} \int_0^T \left[\frac{d}{dt}\left(\eta_\alpha \tau_0 e^{-\lambda_\alpha t}\right)\right]^2 dt \\ &= \sum_{\alpha(\neq 1)} \eta_\alpha^2 \tau_0^2 g(\lambda_\alpha), \end{aligned} \tag{15}$$

where

$$f(\lambda_\alpha) = \frac{1 - e^{-2\lambda_\alpha T}}{2\lambda_\alpha} \quad \text{and} \quad g(\lambda_\alpha) = \frac{1}{2}\lambda_\alpha (1 - e^{-2\lambda_\alpha T}). \tag{16}$$

The set of η_α along with $f(\lambda_\alpha)$ or $g(\lambda_\alpha)$ determine the rate of the system returning to the synchronized state, as measured by $H_1(T)$ or $H_2(T)$, respectively.

The set of η_α are the vector projection of the perturbation onto the right eigenvectors, and the perturbations are in general random numbers that are drawn from a given distribution. Here, we remove the mean of the perturbed natural frequencies with $\delta\omega_0^T u_1 = 0$, and we standardize the norm of ω_0 as $\|\delta\omega_0\|_2 = s$, where the quantity s quantifies the strength of the Dirac delta perturbation. The eigenvalues are sorted in increasing order with $\lambda_1 = 0$. We thus obtain η as $\|\eta\|_2^2 = s^2$, with $\eta_1 = 0$. For a fixed time T, we shall first investigate the best and worst case scenarios of a system's return rate [minimizing or maximizing $H_1(T)$] given this standardization.

In this case, Eq. (12) acquires the form

$$H_1(T) = \sum_{\alpha \geq 2} {\eta_\alpha}^2 {\tau_0}^2 f(\lambda_\alpha).$$

Since $f(\lambda) = \int_0^T e^{-2\lambda t} dt$, its derivative is $f'(\lambda) = -\int_0^T 2te^{-2\lambda t} dt$ and is ≤ 0; hence, $f(\lambda)$ is a strictly monotone decreasing function and $f(+\infty) = 0$. Therefore, to minimize $H_1(T)$, η should meet the following requirements:

$$\eta_\alpha = \begin{cases} 0 & \alpha \in [1, N-1],\ \alpha \in \mathrm{N}^*, \\ s & \alpha = N. \end{cases} \tag{17}$$

Under such circumstances, the minimum value of $H_1(T)$ is

$$H_{1,\min}(T) = \frac{s^2 {\tau_0}^2 (1 - e^{-2\lambda_N T})}{2\lambda_N}. \tag{18}$$

Similarly, we can also obtain the maximum value of $H_1(T)$ as

$$H_{1,\max}(T) = \frac{s^2 {\tau_0}^2 (1 - e^{-2\lambda_2 T})}{2\lambda_2}. \tag{19}$$

We next investigate the best and worst scenarios of a system's return rate to synchronization, after action of a perturbation, by maximizing or minimizing $H_2(T)$. The derivative of $g(\lambda)$ is $g'(\lambda) = \frac{1}{2}\left(1 - e^{-2\lambda T}\right) + \lambda T e^{-2\lambda T}$ and this is a sum of two non-negative terms and hence ≥ 0 with $g(0) = 0$. Thus, $g(\lambda)$ is a strictly monotone increasing function, and to "maximize" $H_2(T)$, η follows from the same form that "minimizes" $H_1(T)$. We thus obtain the maximum value of $H_2(T)$ of

$$H_{2,\max}(T) = \frac{s^2 \lambda_N {\tau_0}^2}{2}(1 - e^{-2\lambda_N T}). \tag{20}$$

Similarly, the minimum value of $H_2(T)$ is

$$H_{2,\min}(T) = \frac{s^2 \lambda_2 {\tau_0}^2}{2}(1 - e^{-2\lambda_2 T}). \tag{21}$$

The above procedure demonstrates that we can determine the best and worst case responses of the system after a perturbation. A local maximization (minimization) occurs when the spatial weights of η (or perturbed natural frequencies) are a linear function of the eigenvector corresponding to the largest (second) eigenvalue.

To illustrate the theoretical results, we have used an Erdos-Renyi (ER) random network to generate a symmetric adjacency matrix and then numerically characterized the corresponding collective dynamics. Each pair of N nodes are connected with the probability P_{ER}. In this work, we consider $N = 200$ and $P_{ER} = 0.2$.

The two response measures, $H_1(T)$ and $H_2(T)$, are shown in Fig. 1 as functions of the coupling strength K. On increasing K, the function $H_1(T)$ continuously decreases and approaches 0, and the corresponding stability of the system increases. The expression of $H_{2,\max}$ is third order sensitive to derivatives, and it preferable to use a third order central difference formulation during numerical simulations. We have investigated the dynamics when the perturbed natural frequencies correspond to the eigenvector u_N. Theoretical results are calculated from Eqs. (18) and (20) and are plotted by a solid line in blue. Numerical results are calculated by definition from Eqs. (5) and (6) and are plotted by a dotted line in orange.

In a high-dimensional system, multistable states exist and the system can migrate from one state to another under large perturbations. The analytic approximation of this work applies for small perturbations of the strongly synchronized regime. To quantify the limitation of the linear approximation adopted in this work, we have investigated the relationship between the performance measures $H_1(T)$ and $H_2(T)$, and the strength of the Dirac delta perturbation, s ($s = \|\delta\omega_0\|_2$), as shown in Fig. 2. From Fig. 2, relatively small values of s ($s < 1.5$) show a very reasonable agreement between the analytically calculated and numerical values. For $s > 1.5$, the difference between analytical and numerical solutions increases with s. In what follows, we set the strength of delta perturbation, s, to 1. We integrate the system under the natural frequencies corresponding to the eigenvector u_N Theoretical results (denoted by Theory) are calculated from Eqs. (18) and (20) and are plotted by a solid line in blue. Numerical results (denoted by Simulation) are calculated by definition from Eqs. (5) and (6) and are plotted by a dotted line in orange.

Additionally, the performance measures H_1 and H_2, under Dirac delta perturbations that minimize/maximize H_1/H_2, and with random perturbations with $s = 1$, are shown in Fig. 3. The y-axis corresponds to the distribution of both measures. When the perturbed natural frequencies correspond to the dominant eigenvector u_N, the system's responses are optimized, represented by $H_{1,\min}$ (in yellow) and $H_{2,\max}$ (in blue), which are obtained from Eqs. (18) and (20), respectively. The other two curves correspond to the worst case scenarios represented by $H_{1,\max}$ (in blue) and $H_{2,\min}$ (in yellow) from Eqs. (19) and (21), respectively. For comparison, numerical results are also calculated according to the original definition from Eqs. (5) and (6) with random perturbations, and are plotted in red.

Note that the Laplacian matrix is a function of both the network graph properties and the synchronized state. In the strong coupling regime, $\cos(\theta_i^{(0)} - \theta_j^{(0)}) \approx 1$. In this case, the Laplacian matrix is approximately

$$\boldsymbol{L}_{ij}^{(0)} = \begin{cases} -K\boldsymbol{A}_{ij} & \text{when } i \neq j, \\ K\sum_k \boldsymbol{A}_{ik} & \text{when } i = j. \end{cases}$$

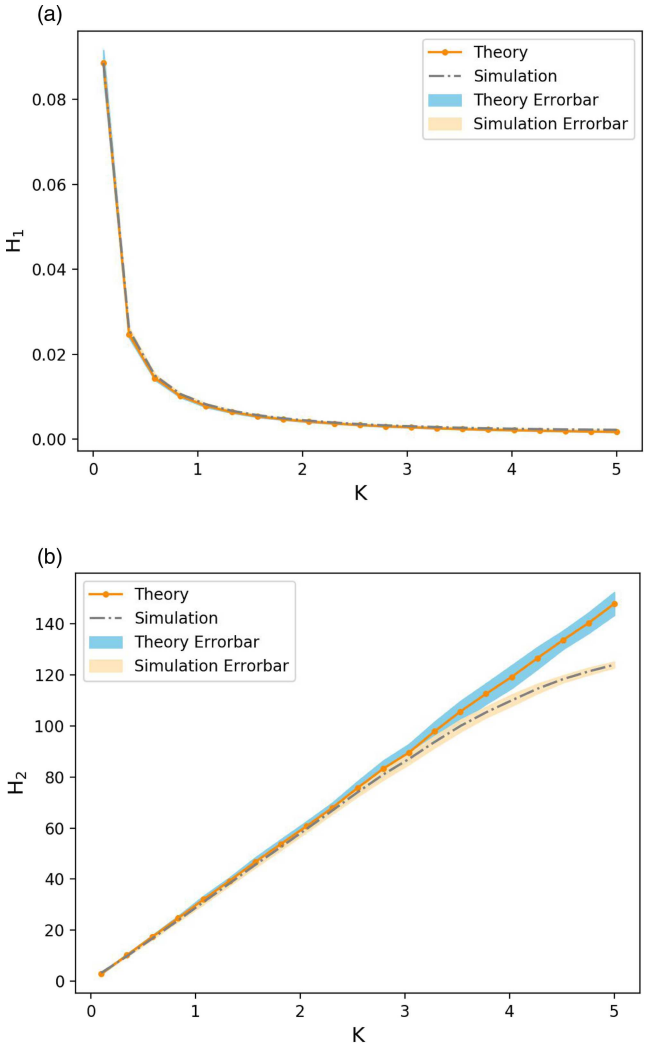

FIG. 1. The two fragility performance measures of $H_1(T)$ and $H_2(T)$ as a function of the coupling strength K. (a) With the increase of K, $H_1(T)$ decreases continuously and approaches 0, and the corresponding system's stability increases. (b) We operate the system's dynamics with the perturbed natural frequencies corresponding to the eigenvector u_N. Theoretical results (denoted by Theory) are calculated from Eqs. (18) and (20) and are plotted by a solid line in blue. Numerical results (denoted by Simulation) are calculated by definition from Eqs. (5) and (6) and are plotted by a dotted line in orange. Here, we use $N = 200$ oscillators, the probability of any edge $P_{ER} = 0.2$, $T = 50$, and results are averaged over 100 times of realizations of ER networks.

This matrix is based solely on network properties. To exhibit the influence of the rewritten Laplacian matrix on both performance measures [compared to the previous one (4)], we introduce the relative error of the two calculation methods, i.e., $H^{(0)}/H$. If the relative error approaches unity, the influence of the synchronized states decreases; otherwise its influence increases. Following previous steps, we calculate $H_{1,\min}^{(0)}$ and $H_{2,\max}^{(0)}$, and find that with increases of the

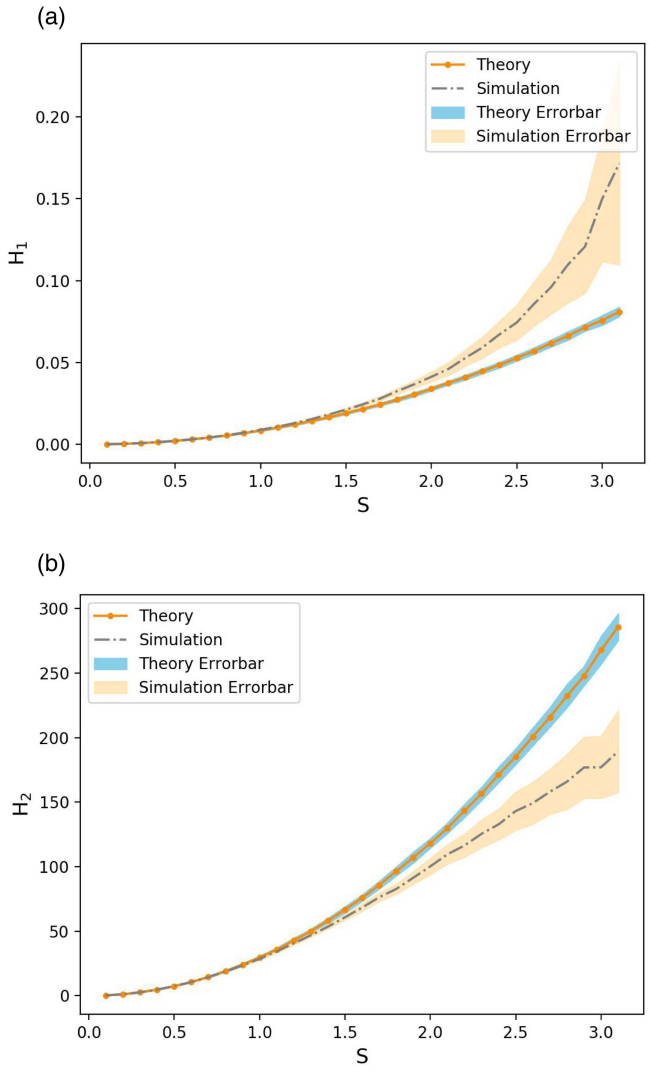

FIG. 2. The two fragility performance measures $H_1(T)$ and $H_2(T)$ as a function of the strength of delta perturbation $s(s = \|\delta\omega_0\|_2)$. With the increase of s, $H_1(T)$ and $H_2(T)$ decrease gradually. We operate the system's dynamics under the perturbed natural frequencies corresponding to the eigenvector u_N. The theoretical results (denoted by Theory) are calculated from Eqs. (18) and (20) and are plotted by a solid line in blue. The numerical results (denoted by Simulation) are calculated by definition from Eqs. (5) and (6) and are plotted by a dotted line in orange. Here, we use $N = 200$ oscillators, the probability of each edge $P_{ER} = 0.2$, $T = 50$, and results are averaged over 100 times of realizations of ER networks.

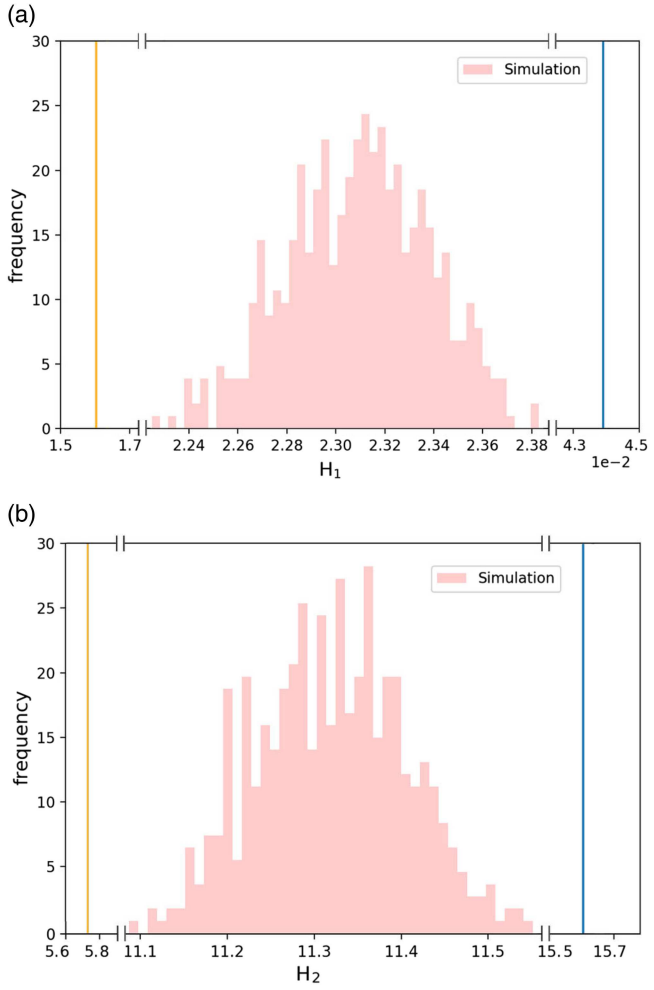

FIG. 3. Performance measures of H_1 and H_2 under the optimized Dirac delta perturbation and with its variation with $s = 1$. y-axis corresponds to the distribution of the two measures. When the perturbed natural frequencies correspond to the dominant eigenvector u_N, the system's responses are optimized, represented with $H_{1,\min}$ (in yellow) and $H_{2,\max}$ (in blue) from Eqs. (18) and (20). The other two lines corresponding the worst case with $H_{1,\max}$ (in blue) and $H_{2,\min}$ (in yellow) from Eqs. (19) and (21). For comparison, Effects of random perturbations on performances are colored in red. Here, we use $N = 200$ oscillators, the probability of each edge $P_{ER} = 0.2$, the coupling strength $K = 1.5$, and $T = 50$.

coupling strength, the influence of the states on H_1 and H_2 gradually decreases, with the ratio $H^{(0)}/H$ approaching unity, as shown in Fig. 4.

IV. STRUCTURAL PERTURBATIONS

In a networked system, the underlying topology is, in general, crucial to the system's states. As shown in Fig. 4, when $K >$ 0.6, the difference between the approximated performances H^0 with $\cos(\theta_i^{(0)} - \theta_j^{(0)}) \approx 1$ and the H of the calculated states vanishes (with $H^{(0)}/H$ approaching 1). Therefore, it is reasonable to neglect the effects of the system's states on the performance metrics given structural perturbations in the strong coupling regime. In this section, we investigate the effects of structural perturbations on $H_1(T)$ and $H_2(T)$ by means of Gersgorin's circle theorem, given perturbed natural frequencies that correspond to the eigenvector u_N. The original network's adjacency matrix is redenoted by $\boldsymbol{P}$ for convenience of explanation, and the structural perturbations are denoted by $\boldsymbol{B}$. The matrix

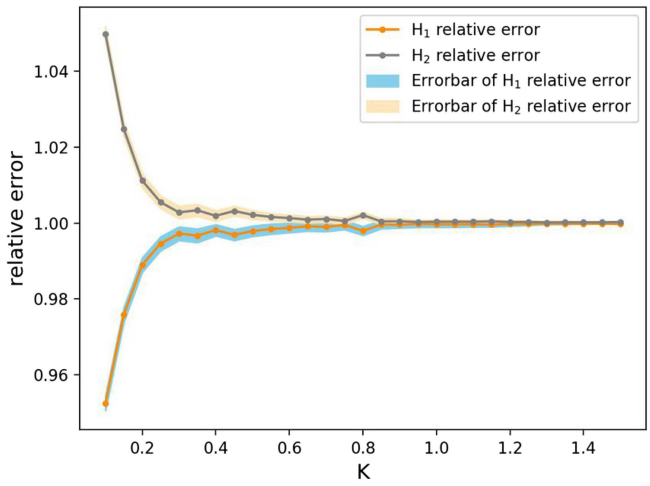

FIG. 4. Effects of synchronized states on Performance measures H_1 and H_2 vary with the coupling strength. The influence is defined as the relative error of the two calculation methods, i.e., $H^{(0)}/H$. With the increasing of coupling strength, the influence of synchronous states on H_1 and H_2 decreases gradually with $H^{(0)}/H$ approaching 1. The value of the relative error related to $H_1(T)$ is colored in orange and the value related to $H_2(T)$ is colored in blue. Here, we use $N = 200$ oscillators, the probability $P_{ER} = 0.2$, $T = 50$, and results are averaged over 100 times of realizations of ER networks.

$\boldsymbol{P}$ includes non-negative elements, while matrix $\boldsymbol{B}$ includes nonpositive elements, and $|\boldsymbol{B}|$ is a subset of $\boldsymbol{P}$. We rewrite the final adjacency matrix as $\boldsymbol{A} = \boldsymbol{P} + \epsilon\boldsymbol{B}$, where $\epsilon\boldsymbol{B}$ represents a structural perturbation term and ϵ quantifies the strength of the perturbation. For the structural perturbation $\epsilon\boldsymbol{B}$, we provide a general theoretical framework for $H_1(T)$ and $H_2(T)$ as a function of structural perturbations, and analyze the relative error between the theoretical and numerical values.

For convenience, we rewrite the Laplacian matrix in terms of $\boldsymbol{P}$ and $\boldsymbol{B}$. Elements of the symmetric matrix $\boldsymbol{L_P}$ are defined as

$$\boldsymbol{L}_{\boldsymbol{P},ij} = \begin{cases} -K\boldsymbol{P}_{ij}\cos(\theta_i^{(0)} - \theta_j^{(0)}) & \text{when } i \neq j, \\ K\sum_k \boldsymbol{P}_{ik}\cos(\theta_i^{(0)} - \theta_k^{(0)}) & \text{when } i = j, \end{cases}$$

while elements of the symmetric matrix $\boldsymbol{L_B}$ are

$$\boldsymbol{L}_{\boldsymbol{B},ij} = \begin{cases} -K\boldsymbol{B}_{ij}\cos(\theta_i^{(0)} - \theta_j^{(0)}) & \text{when } i \neq j, \\ K\sum_k \boldsymbol{B}_{ik}\cos(\theta_i^{(0)} - \theta_k^{(0)}) & \text{when } i = j. \end{cases}$$

Given $\boldsymbol{U} = [u_1, u_2, \ldots, u_N]$, where u_α is the eigenvector corresponding to the αth normalized eigenvalue of $\boldsymbol{L_P}$, we carry out a decomposition to $\boldsymbol{L_A}$ for $\boldsymbol{L_A} \overset{def}{=} \boldsymbol{L_P} + \epsilon\boldsymbol{L_B}$, namely,

$$\boldsymbol{U}^{-1}(\boldsymbol{L_P} + \epsilon\boldsymbol{L_B})\boldsymbol{U} = \boldsymbol{D} + \epsilon\boldsymbol{C},$$

where $\boldsymbol{D} = \mathrm{diag}\{\lambda_1, \lambda_2, \ldots, \lambda_N\}$ and $\boldsymbol{C} = \boldsymbol{U}^{-1}\boldsymbol{L_B}\boldsymbol{U}$ with elements $\boldsymbol{C}_{\alpha\beta} = {u_\alpha}^T\boldsymbol{L_B}u_\beta$.

For a diagonal matrix $\boldsymbol{F}$ defined as

$$\boldsymbol{F}_{ii} = \begin{cases} \epsilon\alpha & i = k, \\ 1 & i \neq k, \end{cases}$$

a similarity transformation of the original matrix is $\boldsymbol{F}\boldsymbol{U}^{-1}(\boldsymbol{P} + \epsilon\boldsymbol{L_B})\boldsymbol{U}\boldsymbol{F}^{-1} = \boldsymbol{D} + \epsilon\boldsymbol{F}\boldsymbol{C}\boldsymbol{F}^{-1}$. The ijth element has the following form as

$$(\boldsymbol{D} + \epsilon\boldsymbol{F}\boldsymbol{C}\boldsymbol{F}^{-1})_{kj} = \begin{cases} \epsilon^2\alpha\boldsymbol{C}_{kj} & j \neq k, \\ \lambda_k + \epsilon\boldsymbol{C}_{kk} & j = k, \end{cases}$$

$$(\boldsymbol{D} + \epsilon\boldsymbol{F}\boldsymbol{C}\boldsymbol{F}^{-1})_{ik} = \frac{1}{\alpha}\boldsymbol{C}_{ik}, \quad i \neq k.$$

According to the Gersgorin circle theorem, the eigenvalue $\lambda_k(\epsilon)$ of the perturbed Laplacian matrix is located in a plane with center $\lambda_i + \epsilon\boldsymbol{C}_{ii}$ and radius r_i. For $i = k$, we have $r_k = \epsilon^2\alpha\sum_{j\neq k}|\boldsymbol{C}_{kj}|$, and for $i \neq k$, $r_i = \epsilon\sum_{j\neq k}|\boldsymbol{C}_{ij}| + \frac{1}{\alpha}|\boldsymbol{C}_{ik}|$. The distance between the centers of circle i and circle k is $|\lambda_i - \lambda_k| - \epsilon|\boldsymbol{C}_{ii} - \boldsymbol{C}_{kk}|$, while the sum of radii is $\epsilon^2\alpha\sum_{j\neq k}|\boldsymbol{C}_{kj}| + \epsilon\sum_{j\neq k}|\boldsymbol{C}_{ij}| + \frac{1}{\alpha}|\boldsymbol{C}_{ik}|$. As $\epsilon \to 0$, we can, by choosing a sufficiently large α, ensure that these two circles do not intersect with each other and $\boldsymbol{C}_{kk}$ is solely determined by one circle corresponding to index k. This indicates that $|\lambda_k(\epsilon) - \lambda_k - \epsilon\boldsymbol{C}_{kk}| \leq \epsilon^2\alpha\sum_{j\neq k}|\boldsymbol{C}_{kj}|$, and the perturbed eigenvalue $\lambda_k(\epsilon)$ becomes

$$\lambda_k(\epsilon) = \lambda_k + \epsilon{u_k}^T\boldsymbol{L_B}u_k + O(\epsilon^2).$$

When the perturbed natural frequencies correspond to the eigenvector u_N associated with the largest eigenvalue, and $\delta{\omega_0}^T = \sum_{r=1}^N \eta_r {u_r}^T$, the performance measures $H_1(T)$ and $H_2(T)$ are redefined as a function of T as

$$H_{1,est}(T) = \sum_{\alpha\geq 2} {\eta_\alpha}^2{\tau_0}^2\frac{1 - \mathrm{e}^{-2T\lambda_\alpha(\epsilon)}}{2\lambda_\alpha(\epsilon)}, \tag{22}$$

$$H_{2,est}(T) = \sum_{\alpha\geq 2} {\eta_\alpha}^2{\tau_0}^2\frac{\lambda_\alpha(\epsilon)}{2}(1 - \mathrm{e}^{-2T\lambda_\alpha(\epsilon)}). \tag{23}$$

Effects of structural perturbations on the performance measures H_1 and H_2, as a function of disconnection probability P, are shown in Fig. 5. Edges are disconnected with probability P, the smaller P corresponds to the smaller ϵ above. The structural perturbation is operated numerically with P, and this operation refers to the term $\epsilon\boldsymbol{B}$ in the analytical part. When $P = 0$, the performance measures H_1 and H_2 indicate the system's responses without any structural perturbations but solely with the perturbed natural frequency. When $P > 0$, we randomly perturb the network 100 times. For each kind of perturbation, we integrate the system and calculate the corresponding performance measures. Mean theoretical results of $H_1(T)$ and $H_2(T)$ with 100 random perturbations are obtained from Eqs. (22) and (23) and are plotted in orange. Mean numerical results are obtained from Eqs. (5) and (6) and are plotted in gray. The shaded regions indicate their standard deviations. The system is operated given the optimized natural frequencies corresponding to the eigenvector u_N in the regime of strong coupling.

We approximate the theoretical results of $H_1(T)$ and $H_2(T)$ after a perturbation. To evaluate the difference between the approximated values and real solutions, we quantify the similarity of H_1 and H_2 as

$$\mathrm{Similarity}(H_1) = \frac{H_{1,est} - H_{1,before}}{H_{1,after} - H_{1,before}},$$

$$\mathrm{Similarity}(H_2) = \frac{H_{2,est} - H_{2,before}}{H_{2,after} - H_{2,before}}.$$

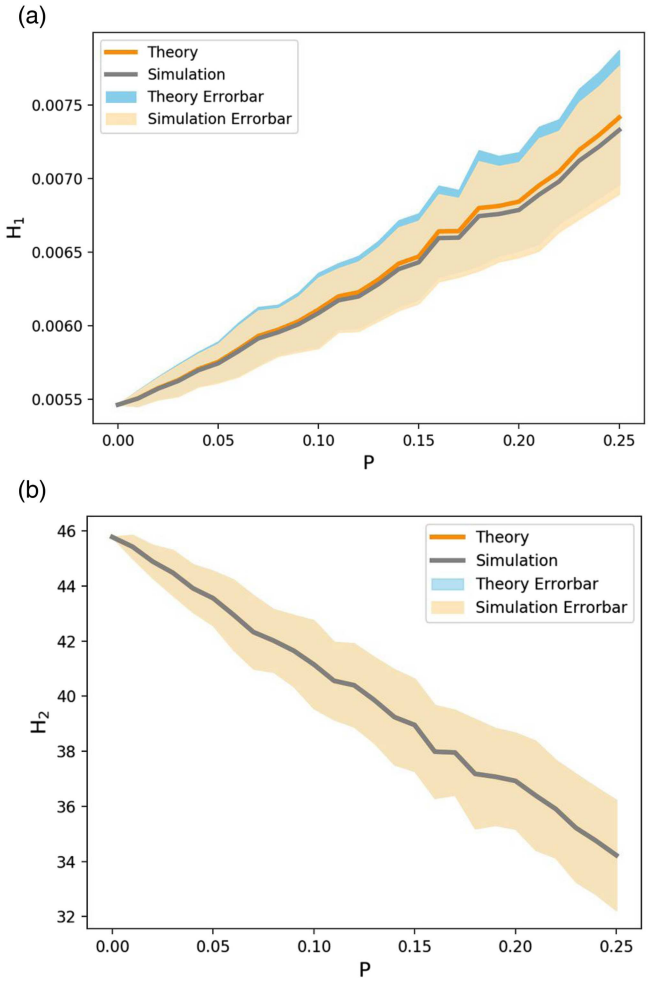

FIG. 5. Effects of structural perturbations on the two performance measures H_1 and H_2 as a function of disconnection probability P. Given one disconnection probability P, we perturb the network 100 times. For each kind of perturbation, we integrate the system and calculate the corresponding performance measures. Theoretical mean results of $H_1(T)$ and $H_2(T)$ with 100 randomly perturbations are obtained from Eqs. (22) and (23) and are colored in orange. Numerical mean results are obtained from Eqs. (5) and (6) and are colored in gray. The shades show their standard deviations. The system is operated given the optimized natural frequencies corresponding to the eigenvector u_N in the regime of the strong coupling regime. Here, we use $N = 200$ oscillators, the interconnection probability $P_{ER} = 0.2$, the coupling strength K = 1.5, and $T = 50$.

Here, $H_{1/2,before}$ and $H_{1/2,after}$ are obtained from the original nonlinear function Eqs. (5) and (6). $H_{1/2,before}$ is the numerical result under the condition that the structure has not been perturbed, and $H_{1/2,after}$ corresponds to the perturbation of system structure. The difference between the approximated values and the actual solutions is shown in Fig. 6. The similarity values remain almost consistent and are independent of P. But the standard deviations decrease with the increases of P.

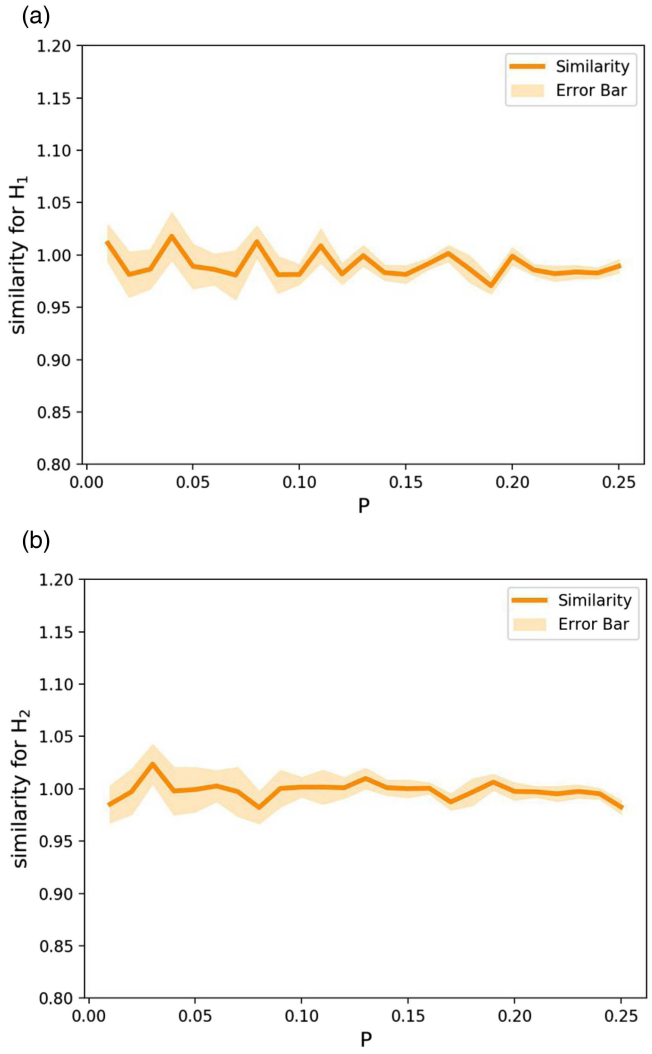

FIG. 6. The difference between the approximated values and real solutions is represented by the similarity. The mean similarity remains a high value given different P values, the saddle shows the corresponding variation given different perturbations. Given one disconnection probability P, we perturb the network 100 times. For each kind of perturbation, we integrate the system and calculate the corresponding performance measures. Theoretical mean results of $H_1(T)$ and $H_2(T)$ with 100 randomly perturbations are obtained from Eqs. (22) and (23), while numerical mean results are obtained from Eqs. (5) and (6), and the similarity is colored in orange. The light yellow shades show their standard deviations. The system is operated given the optimized natural frequencies corresponding to the eigenvector u_N in the regime of the strong coupling regime. Here, we use $N = 200$ oscillators, the interconnection probability $P_{ER} = 0.2$, the coupling strength K = 1.5, and $T = 50$.

V. CONCLUSIONS

Using two performance measures, we have investigated the response of the synchronized state to perturbations of (i) the natural frequencies and (ii) structural perturbations. We have shown that the

best and worst case scenarios of a system's response depend on the scalar product of the perturbations of the natural frequency and the eigenmodes of the system's Laplacian matrix. Given Dirac delta perturbations, we have shown that when the perturbations correspond to the dominant eigenmode, their impacts on the system are minimized. Our results remain consistent with recent results from different perspectives, e.g., via a synchrony alignment function,[19,20] the robustness of synchrony via generalized Kirchhoff indices.[15]

For structural perturbations, we have conducted a spectral perturbation analysis of the performance measures for phases and frequencies. Based on the methods presented, we have approximated the effects of network modifications on a system's robustness. Additionally, we have conducted a number of simulations to test our theory. Our results reveal the combined impacts of Dirac delta perturbations, structural perturbations, and topological features on system's stabilities, and deepen our understanding of stability control, and it is also straightforward to extend our results to optimize synchronization in complex clustered networks.[21–23]

ACKNOWLEDGMENTS

We acknowledge the National Key R&D Program of China (No. 2018YFB0904500), the Natural Science Foundation of Shanghai, Shanghai Pujiang Program, the Program for Professor of Special Appointment (Eastern Scholar) at Shanghai Institutions of Higher Learning and by NSFC 269 (No. 11701096), the National Science Foundation of China under Grant No. 61773125.

REFERENCES

[1] S. H. Strogatz, "From Kuramoto to Crawford: Exploring the onset of synchronization in populations of coupled oscillators," Physica D **143**(1–4), 1–20 (2000).
[2] J. A. Acebrón, L. L. Bonilla, C. J. P. Vicente, F. Ritort, and R. Spigler, "The Kuramoto model: A simple paradigm for synchronization phenomena," Rev. Mod. Phys. **77**(1), 137 (2005).
[3] F. A. Rodrigues, T. K. D. M. Peron, P. Ji, and J. Kurths, "The Kuramoto model in complex networks," Phys. Rep. **610**, 1–98 (2016).
[4] J. Pantaleone, "Stability of incoherence in an isotropic gas of oscillating neutrinos," Phys. Rev. D **58**(7), 073002 (1998).
[5] Y. Yang and A. E. Motter, "Cascading failures as continuous phase-space transitions," Phys. Rev. Lett. **119**(24), 248302 (2017).
[6] K. Wiesenfeld, P. Colet, and S. H. Strogatz, "Synchronization transitions in a disordered Josephson series array," Phys. Rev. Lett. **76**(3), 404 (1996).
[7] P. Ji, T. K. D. M. Peron, P. J. Menck, F. A. Rodrigues, and J. Kurths, "Cluster explosive synchronization in complex networks," Phys. Rev. Lett. **110**(21), 218701 (2013).
[8] A. Pikovsky, M. Rosenblum, and J. Kurths, *Synchronization: A Universal Concept in Nonlinear Sciences* (Cambridge University Press, 2003), Vol. 12.
[9] A.-L. Barabási and R. Albert, "Emergence of scaling in random networks," Science **286**(5439), 509–512 (1999).
[10] S. Takeuchi and E. Kuramoto, "Thermally activated motion of a screw dislocation in a model bcc crystal," J. Phys. Soc. Jpn. **38**(2), 480–487 (1975).
[11] A. Arenas, A. Díaz-Guilera, J. Kurths, Y. Moreno, and C. Zhou, "Synchronization in complex networks," Phys. Rep. **469**(3), 93–153 (2008).
[12] B. Bamieh, M. R. Jovanovic, P. Mitra, and S. Patterson, "Coherence in large-scale networks: Dimension-dependent limitations of local feedback," IEEE Trans. Automat. Contr. **57**(9), 2235–2249 (2012).
[13] E. Tegling, B. Bamieh, and D. F. Gayme, "The price of synchrony: Evaluating the resistive losses in synchronizing power networks," IEEE Trans. Control Netw. Syst. **2**(3), 254–266 (2015).
[14] B. K. Poolla, S. Bolognani, and F. Dörfler, "Optimal placement of virtual inertia in power grids," IEEE Trans. Automat. Contr. **62**(12), 6209–6220 (2017).
[15] M. Tyloo, T. Coletta, and Ph. Jacquod, "Robustness of synchrony in complex networks and generalized Kirchhoff indices," Phys. Rev. Lett. **120**(8), 084101 (2018).
[16] L. M. Pecora and T. L. Carroll, "Master stability functions for synchronized coupled systems," Phys. Rev. Lett. **80**(10), 2109 (1998).
[17] P. J. Menck, J. Heitzig, N. Marwan, and J. Kurths, "How basin stability complements the linear-stability paradigm," Nat. Phys. **9**(2), 89 (2013).
[18] P. Ji, W. Lu, and J. Kurths, "Stochastic basin stability in complex networks," Europhys. Lett. **122**(4), 40003 (2018).
[19] D. Taylor, P. S. Skardal, and J. Sun, "Synchronization of heterogeneous oscillators under network modifications: Perturbation and optimization of the synchrony alignment function," SIAM J. Appl. Math. **76**(5), 1984–2008 (2016).
[20] S. P. Sebastian, T. Dane, and S. Jie, "Optimal synchronization of complex networks," Phys. Rev. Lett. **113**(14), 144101 (2014).
[21] X. Wang, L. Huang, Y.-C. Lai, and C. H. Lai, "Optimization of synchronization in gradient clustered networks," Phys. Rev. E **76**(5), 056113 (2007).
[22] L. Huang, Y.-C. Lai, and R. A. Gatenby, "Optimization of synchronization in complex clustered networks," Chaos **18**(1), 013101 (2008).
[23] L. Huang, Y.-C. Lai, and R. A. Gatenby, "Alternating synchronizability of complex clustered networks with regular local structure," Phys. Rev. E **77**(1), 016103 (2008).